J. Phys. Chem. A **1999,** *103,* 7907−7911

Structure and [2+2] Cycloreversion of the Cyclobutane Radical Cation

Olaf Wiest[†]

Department of Chemistry and Biochemistry, University of Notre Dame, Notre Dame, Indiana 46556-5670

Received: June 11, 1999; In Final Form: August 2, 1999

The [2+2] cycloreversion reaction of the cyclobutane radical cation was studied using high-level MO and DFT methods. Three distinct, but energetically very similar, structures are located for the cyclobutane radical cation: a parallelogram that corresponds to the minimum on the Jahn−Teller surface, a rhombus, corresponding to a transition structure connecting two parallelograms, and a rectangle that is a second-order saddle point. Intrinsic reaction coordinate calculations show that the reaction proceeds in a concerted fashion. The calculated reaction mode is not consistent with a putative acyclic intermediate, but rather shifts the two ethylene fragments relative to each other. The transition structure connects the product complex to the parallelogram structure of the cyclobutane radical cation. The overall thermochemistry calculated by the QCISD(T)//QCISD and the B3LYP methods are in good agreement with the available experimental data. It is shown that the experimental hyperfine coupling constants do not imply a puckered structure, as claimed earlier. The electronic structure and magnetic properties of the transition structure are elucidated by NICS calculations.

Introduction

The [2+2] cycloreversion/cycloaddition reaction of cyclobutanes is one of the most important electron transfer catalyzed (ETC) pericyclic reactions. It was not only the first reaction to be recognized as having a radical cationic pathway,[1] but has also important biological implications in the ETC repair of the cyclobutane thymine dimer in UV damaged DNA, catalyzed by the enzyme DNA photolyase.[2] In addition, several substituted cyclobutane radical cations such as the quadricyclane[3] and the pagodane[4] radical cations undergo [2+2] cycloreversion and attracted considerable theoretical interest. Finally, the possibility of catalyzing a symmetry-forbidden cycloaddition through electron transfer opens new synthetic pathways in organic chemistry. Consequently, the electron transfer catalyzed cycloreversion of substituted cyclobutanes has been studied extensively over the last two decades.[5] Most mechanistic studies center around the question which of the two pathways shown in Figure 1 is followed: a concerted pathway with a single transition state or stepwise pathway involving an acyclic tetramethylene radical cation.

The most simple case, the [2+2] cycloreversion of the parent cyclobutane radical cation $\mathbf{1}^{\bullet+}$, as well as the product complex $\mathbf{3}^{\bullet+}$ have been studied by Ono et al.,[6] Doepker et al.,[7] and others using various experimental methods. Theoretical studies of the parent system by the groups of Bauld,[8] Lunell,[9] Glukhovtsev,[10] and others[11] did not yield conclusive evidence for or against the involvement of an acyclic intermediate. In a careful theoretical study, Jungwirth et al.[12] optimized a number of possible structures for $\mathbf{1}^{\bullet+}$, the transition structure for cycloreversion and the product complex $\mathbf{3}^{\bullet+}$ of ethylene and the ethylene radical cation at the UMP2/6-31G* level of theory. The authors of this study did not locate a minimum corresponding to the previously postulated[13] tetramethylene radical cation and concluded therefore that the cycloreversion or isomerization of $\mathbf{1}^{\bullet+}$ "does not appear to proceed via a tetramethylene radical cation".[12] It was also noted that the highly spin contaminated UHF wave function makes the use of UHF and UMP2 calculations for these radical cations problematic.[14]

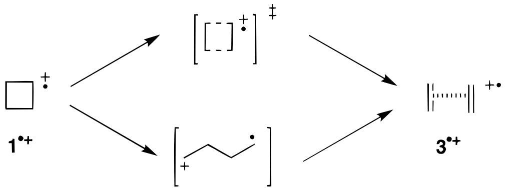

Figure 1. Possible pathways for the cycloreversion of $\mathbf{1}^{\bullet+}$.

In light of the importance of the ETC cycloreversion for organic and bioorganic chemistry, a further theoretical investigation of the reaction is worthwhile. In this paper, high-level quantum mechanical methods are used to answer the following questions: (i) What is the structure of $\mathbf{1}^{\bullet+}$? (ii) Is the tetramethylene radical cation part of the reaction pathway? (iii) What is the electronic nature of the transition structure? and (iv) What are appropriate levels of theory for this reaction?

Computational Methodology

Electron correlation in radical ions can generally be treated using either single- or multideterminant approaches. While the choice of the active space for CASSCF calculations is often problematic for radical ions,[15] the QCISD(T) method has been shown to recover most of the electron correlation in multireference problems.[16] Therefore, we performed QCISD(T)/6-311G** calculations on QCISD/6-31G* optimized geometries (hereafter denoted as QCISD(T)//QCISD) to obtain reliable reference values. In addition, UHF and MP2, BLYP and Becke3LYP calculations using the 6-31G* basis set have been performed. These computationally efficient, gradient-corrected and hybrid DFT methods have been shown to yield accurate results for a large number of different systems,[17] including open shell systems and ion−molecule complexes,[18] without encountering the problems associated with spin contamination.[19] More recently, the use of hybrid DFT methods has, however, been questioned due to their bias toward delocalized structures.[20]

[†] E-mail: owiest@nd.edu. Fax: (219) 631 6652.

10.1021/jp991917r CCC: $18.00

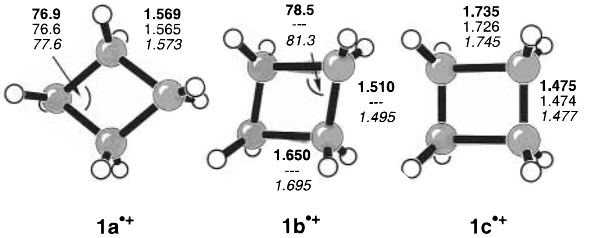

Figure 2. Rhombic (**1a**$^{\bullet+}$, left), parallelogram (**1b**$^{\bullet+}$, middle) and rectangular (**1c**$^{\bullet+}$, right) structures of **1**$^{\bullet+}$ with selected geometric parameters (bold: QCISD; plain: MP2; italics: Becke3LYP).

Comparison of these results with the ones from the reference QCISD(T)//QCISD calculations then allows a validation of the UHF, MP2, and DFT methods and provides insights into their applicability for the calculation of radical cationic systems.

All calculations were performed using the G94 series of programs.[21] The stationary points reported have been fully optimized and characterized by harmonic frequency analysis. All reported energies, except the data from the IRC calculations, are corrected for zero-point vibrational energies obtained at the same level through frequency calculations. Nuclear independent chemical shifts (NICS) were calculated at the B3LYP/6-311+G** level of theory using the GIAO method as implemented in G94.

Results and Discussion

The cyclobutane radical cation **1**$^{+\bullet}$ is subject to a first and potentially a second-order Jahn−Teller distortion which should lead to one minimum and one transition structure with a lower symmetry than **1** itself. Four structures, the rhombus **1a**$^{\bullet+}$ and the rectangle **1c**$^{\bullet+}$ as well as a kite and a trapezium structure have been studied by Jungwirth et al. at levels up to QCISD(T)/6-31G*//UMP2/6-31G*.[12] Because a spin contamination of $S^2 < 0.77$ was obtained for the UHF wave functions, the UMP2 level was considered as satisfactory for geometry optimizations. Because of the concerns about the accuracy of the UMP2 method mentioned above and to gain further insight into the performance of the different methods discussed here, the four structures discussed above and a parallelogram **1b**$^{\bullet+}$ were fully optimized at the UHF, MP2, QCISD, BLYP, and Becke3LYP levels of theory. Figure 2 shows the structures **1a**$^{\bullet+}$−**1c**$^{\bullet+}$ together with selected geometrical data. Results for the reaction energetics are summarized in Table 1.

For the rhombic **1a**$^{\bullet+}$, which was predicted to be a minimum in the UMP2 calculations,[12] the DFT and the correlated MO methods yield very similar results for the geometry. The calculated C−C bond length of 1.563−1.573 Å is typical for a C−C single bond, indicating that the SOMO is totally delocalized. The correlated MO based methods all predict **1a**$^{\bullet+}$ to be the most stable of the structures listed above, whereas the DFT methods predict it to be negligibly higher in energy than **1b**$^{\bullet+}$ after correction for zero-point energy. Interestingly, both the DFT and the QCISD reference calculations predict one imaginary frequency corresponding to an in-plane distortion for **1a**$^{\bullet+}$. It does therefore not correspond to a minimum as predicted by the UMP2 calculations, but rather to a transition structure connecting two parallelograms **1b**$^{\bullet+}$. Furthermore, the normal mode leading to a ring puckering was found to have a small positive frequency at all levels.

Following the imaginary frequency in **1a**$^{\bullet+}$ leads to the C_{2h} symmetric parallelogram **1b**$^{\bullet+}$, which corresponds to a minimum on the hypersurface and was not calculated previously as a stationary point. The extent of the bond length alteration of the C−C single bond predicted at the Becke3LYP level is 0.2 Å, significantly larger than the value of 0.14 Å calculated at the QCISD level of theory. At the QCISD(T)//QCISD and the Becke3LYP levels, the activation energy for the interconversion of two parallelograms via transition structure **1a**$^{\bullet+}$ is extremely low and essentially disappears after correction for zero-point energy. It is noteworthy that **1b**$^{\bullet+}$ is not a stationary point at the UHF level of theory and collapses to **1a**$^{\bullet+}$ at the UMP2 level.

The rectangular structure **1c**$^{\bullet+}$ results from the distortion of the D_{4h} structure along the b_{2g} mode. The QCISD(T)/QCISD and DFT methods predict this structure to be energetically very close to **1a**$^{\bullet+}$ and **1b**$^{\bullet+}$, whereas the MP2 method predicts it to be 2.1 kcal/mol higher in energy than **1a**$^{\bullet+}$. This energy difference is larger than the 1.9 kcal/mol calculated earlier for the energy difference of **1a**$^{\bullet+}$ and the puckered rectangular structure,[12] thus providing an estimate for the driving force of ring puckering at this level. The UHF method predicts **1c**$^{\bullet+}$ to be more stable than **1a**$^{\bullet+}$ by the relatively large margin of −2.9 kcal/mol, but higher in energy than the global minimum for the cyclobutane radical cation in the trapezoid form identified earlier.[12] Frequency analysis at the QCISD and the DFT levels of theory show that **1c**$^{\bullet+}$ has two imaginary frequencies corresponding to in-plane distortions to **1a**$^{\bullet+}$ and **1b**$^{\bullet+}$. The prediction of a planar structure for **1c**$^{\bullet+}$ is again in contrast to the MP2 results that give a small negative frequency for the ring puckering motion of **1c**$^{\bullet+}$.

The overall picture of the hypersurface of the cyclobutane radical cation as obtained by the QCISD(T) and the hybrid and gradient-corrected DFT methods is with **1b**$^{\bullet+}$ as the minimum, **1a**$^{\bullet+}$ as a transition structure and **1c**$^{\bullet+}$ as a second-order saddle point qualitatively quite different from the UMP2 surface. Although the energy differences obtained here are even lower than the ones obtained at the UMP2 level, the inability of the UMP2 method to locate the minimum on the surface and to correctly represent the characteristics of the stationary points is reason for concern about the applicability of this method even for weakly spin contaminated species. The good agreement between the results from the B3LYP calculations with the ones from the QCIS(T)//QCISD reference level shows that despite earlier concerns, hybrid DFT methods appear to give good

TABLE 1: Zero-Point-Corrected Absolute Energies for the Rhombic Cyclobutane Radical Cation 1a$^{\bullet+}$ and Relative Energies for 1b$^{\bullet+}$−1c$^{\bullet+}$, Transition Structure 2$^{\bullet+}$ and Product Complex 3$^{\bullet+}$ and the Number of Imaginary Frequencies (in parentheses)

method	E_{SCF}(**1a**$^{\bullet+}$) (hartrees)	E_{rel}(**1b**$^{\bullet+}$) (kcal/mol)	E_{rel}(**1c**$^{\bullet+}$) (kcal/mol)	E_{rel}(**2**$^{\bullet+}$) (kcal/mol)	E_{rel}(**3**$^{\bullet+}$) (kcal/mol)
UHF	−155.648 28 (2)		−2.94 (1)	0.5 (1)	−10.1 (0)
UMP2	−156.158 36 (0)		2.14 (2)	16.0 (1)	11.6 (0)
QCISD(T)//UMP2[a]	−156.222 27 (0)		1.1 (2)	13.1 (1)	4.1 (0)
QCISD(T)/QCISD	−156.340 88 (1)	0.03 (0)	0.84 (2)	13.7 (1)	5.8 (0)
BLYP	−156.662 44 (1)	−0.19 (0)	−0.39 (2)	13.9 (1)	−0.9 (0)
Becke3LYP	−156.755 74 (1)	−0.02 (0)	−0.16 (2)	14.8 (1)	2.4 (0)

[a] From ref 12, using the 6-31G* basis set and ZPE correction from MP2/6-31G* calculations.

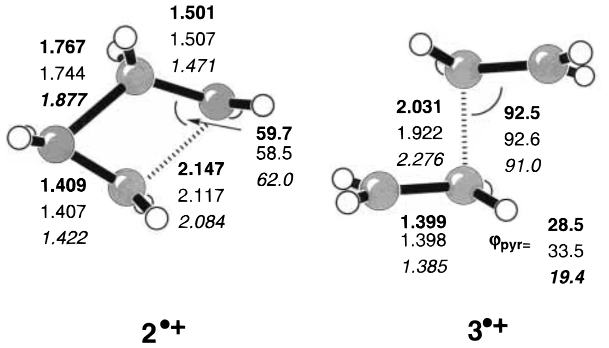

Figure 3. Transition structure **2**$^{\bullet+}$ (left) and product complex **3**$^{\bullet+}$ (right) for the cycloreversion of **1**$^{\bullet+}$ with selected geometric parameters (bold: QCISD; plain: MP2; italics: Becke3LYP).

results for the calculation of radical cations. It should, however, be noted that the energy differences between the various species are too small to be chemically relevant.

All structures calculated here are predicted to be planar. This is apparently in disagreement with the ESR experiments by Iwasaki and co-workers who interpreted the observation of two different hyperfine coupling constants (hfcc) of 49 and 14 G as indicative of a puckered structure.[22] Calculation of the hfcc of **1b**$^{\bullet+}$ at the B3LYP/6-311+G** level of theory gave values of 20.9 and 2.9 G. While the agreement between theory and experiment is, not surprising for a highly flexible structure such as **1**$^{\bullet+}$, only of a qualitative nature, it clearly demonstrates the different hybridization of the carbons in the parallelogram structure **1b**$^{\bullet+}$ is sufficient to induce two quite different hyperfine coupling constants without requiring a puckered ring structure.

The transition structure for the cycloreversion, **2**$^{\bullet+}$, is shown in Figure 3 left. The D_{2h} or C_{2v} symmetry of **1a**$^{\bullet+}$, **1c**$^{\bullet+}$, and **1b**$^{\bullet+}$, is here reduced to a C_s symmetry. The calculated transition structure is quite asynchronous with one bond stretched by 13−19% and the other bond stretched by 32−37% as compared with a normal C−C single bond. This asynchronicity is less pronounced in the structure obtained from the B3LYP calculation than the one from the QCISD and MP2 computations. The structures of **2**$^{\bullet+}$ and **3**$^{\bullet+}$ were already discussed earlier by Jungwirth et al.[12] and our results are in agreement with the structures obtained there. The calculated activation energies demonstrate the power of electron transfer catalysis. The Woodward−Hoffmann forbidden [2+2] cycloreversion of the neutral cyclobutane has an activation energy of 62.5 kcal/mol.[23] Thus, electron transfer catalysis lowers the activation barrier of the reaction by almost 50 kcal/mol! At the same time the results from the UHF calculations, which predict essentially no barrier at all, show again the importance of a proper inclusion of electron correlation into accurate calculations of radical ions.

The product of the reaction in the gas phase, the ethylene−ethylene radical cation complex **3**$^{\bullet+}$, is shown in Figure 3 on the right. Although the carbon−carbon bond in this complex is relatively long, the connecting carbons are considerably pyramidalized. At the best level of theory used here, the reaction of **1**$^{\bullet+}$ to **3**$^{\bullet+}$ is endothermic by 5.8 kcal/mol. This value is bracketed by the MP2 and the B3LYP results. In comparison to the QCISD(T)/QCISD data, the UHF and the BLYP methods do not give reliable results. The overall thermochemistry of the [2+2] cycloreversion of the cyclobutane radical cation to separated ethylene and the ethylene radical cation is also well reproduced by the calculations. The reaction enthalpy for this reaction can be deduced from available experimental data as 34.7 kcal/mol.[24] The QCISD(T)/QCISD and B3LYP calculations predict reaction energies of 32.7 and 33.9 kcal/mol, respectively.[25]

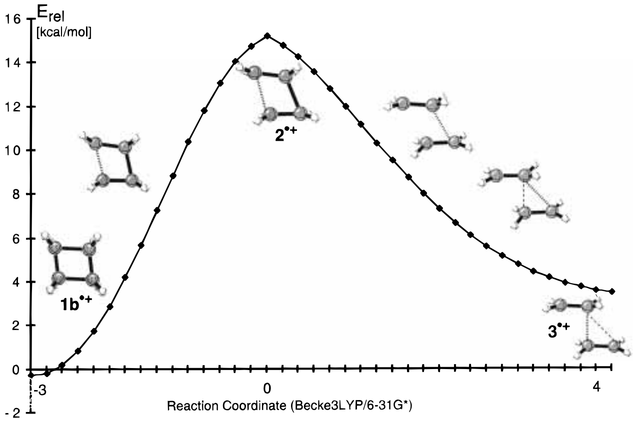

Figure 4. IRC calculation starting from **2**$^{\bullet+}$.

It is also noteworthy that **3**$^{\bullet+}$ closely resembles the MCSCF/STO-3G transition structure for the stepwise dimerization of neutral ethylene,[26] leading to the tetramethylene diradical. An acyclic tetramethylene radical cation intermediate has been proposed earlier for the cycloreversion of both parent and substituted cyclobutanes. In case of the [2+2] cycloreversion of the cyclobutane thymine dimer radical cation, such an intermediate could be trapped with an intramolecular probe.[27] Extensive studies of many different possible structures performed by Jungwirth et al.[12] did not locate a minimum corresponding to such an acyclic intermediate. Although this is strong circumstantial evidence, it does not rigorously exclude the involvement of a tetramethylene radical cation in the reaction pathway, especially since already the neutral tetramethylene diradical proved to be an elusive structure.[28] Since the results from the Becke3LYP calculations are fairly close to the ones from the QCISD(T)//QCISD calculations, this method was used to investigate the complete reaction pathway by an intrinsic reaction coordinate (IRC) calculation, following the imaginary frequency in **2**$^{\bullet+}$. These calculations provide a more direct way to test whether the transition structure connects directly to the product **3**$^{\bullet+}$. Figure 4 shows the results of the IRC following together with the 6 out of a total of 38 calculated structures.

These results clearly show that the reaction proceeds from **2**$^{\bullet+}$ to **3**$^{\bullet+}$ without the involvement of an intermediate, thus demonstrating the concerted mechanism of the reaction. In the reverse direction, **2**$^{\bullet+}$ connects to the parallelogram structure **1b**$^{\bullet+}$. This structure also resembles the calculated transition structure most closely. The transition structure **2**$^{\bullet+}$ is computed to be approximately halfway along the intrinsic reaction coordinate. This is in accordance with the small endothermicity of the reaction. It can also be seen in Figure 4 that the mode of ring opening is very different from the one expected for a reaction involving a tetramethylene radical cation. Instead of a consecutive breaking of the two bonds, the two ethylene fragments shift parallel to each other. The 1,2- and 3,4-bonds break in an asymmetric fashion and form the new 1,3-bond in the product complex. This bond-breaking/bond-forming mode is not in agreement with a putative tetramethylene radical cation intermediate, but rather resembles the transition structure for a [2_s+2_s] cycloreversion.

According to the Woodward−Hoffmann rules, the neutral [2_s+2_s] cycloreversion has an antiaromatic transition state for the ground state reaction of **1**. In order to obtain insights into the electronic structure of the transition structure for the radical

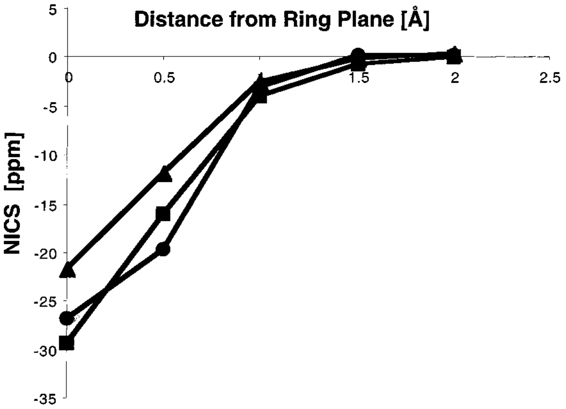

Figure 5. Plot of NICS values (Becke3LYP/6-311+G**) for **1a**$^{•+}$ (■), **1b**$^{•+}$ (▲), and **2**$^{•+}$ (●) as a function of distance to the ring plane.

ionic reaction, we investigated the aromaticity of **2**$^{•+}$ using the NICS calculations as a probe.[29] The comparison of the NICS calculations of **2**$^{•+}$ and **1b**$^{•+}$ as a function of the distance from the ring plane is shown in Figure 5. Not surprising for the small cyclobutane ring, the probe experiences a strong upfield shift due to the local shielding of the nearby σ bonds when positioned in the ring plane. This shielding decays rapidly as the distance between the probe and the ring plane increases. The decay calculated for the transition structure **2**$^{•+}$ and the minimum **1b**$^{•+}$ is essentially identical. This indicates that the electronic structure of **2**$^{•+}$ is neither aromatic or antiaromatic, and that the π-character of the double bonds is not yet very developed in the transition structure.

Summary and Outlook

The reaction pathway of the [2+2]-cycloreversion of the cyclobutane radical cation was studied by an number of high-level theoretical methods. The results of our study complement earlier work by Jungwirth et al.[12] in that they provide closer insight into the geometric, electronic, and magnetic characteristics of the stationary points on the hypersurface, thus providing a connection with the available experimental data. At the best level of theory used in this study, the three possible structures of the cyclobutane radical cation are essentially identical in energy. Calculation of the hyperfine coupling constants demonstrates that the experimentally observed values do not imply a puckered structure, but rather can be explained by differences in hybridization in the **1b**$^{•+}$. The calculated IRC connects the parallelogram structure **1b**$^{•+}$, which was not described earlier, via a single transition structure **2**$^{•+}$ to the product complex **3**$^{•+}$. This reaction pathway does not involve an acyclic intermediate and the transition structure is nonaromatic. The reaction has an activation energy of 13.7 kcal/mol and is endothermic by 5.8 kcal/mol at the QCISD(T)//QCISD level of theory. The experimental thermochemistry of the reaction is well reproduced by the B3LYP and QCISD(T)//QCISD calculations. These results would support the concerted mechanism proposed for the cycloreversion of 1,2 diaryl cyclobutanes.[5a,30] It should be pointed out, however, that substituents on the cyclobutane may easily alter the mechanism by stabilization of an acyclic intermediate on a very flat energy hypersurface. This is likely to be the case for the cycloreversion of the cyclobutane thymine dimer.[23] Comparison of the results from the UHF with the ones from the QCISD(T)//QCISD reference calculations show that the UHF methods is not adequate for the study of the cyclobutane radical cation. The MP2 calculations perform better, but failed to locate the parallelogram structure **1b**$^{•+}$ and provide a qualitatively quite different picture of the potential energy hypersurface. Although the energy differences are too small to be chemically relevant in this case, the discrepancies between the UMP2 calculations on the one hand and the QCISD(T)/QCISD reference calculations on the other caution against the use of the UMP2 method for the calculation of radical ions even when the spin contamination of the underlying Hartree−Fock wave function is low. Finally, the results from the computationally more efficient Becke3LYP method compare quite favorably with the ones from the reference QCISD(T)/QCISD calculations and recent concerns about the applicability of hybrid DFT methods to the calculation of hydrocarbon radical cations do not apply here. These findings encourage the study of these chemically and biochemically more important, substituted cases such as the cyclobutane thymine dimer by Becke3LYP calculations. These studies are currently in progress and will be reported separately.

Acknowledgment. The financial support by the National Institutes of Health (Grant CA73775) and the Volkswagen Foundation (Grant I/72 647) is gratefully acknowledged. I am also grateful to the Office of Information Technologies at the University of Notre Dame and the National Center for Supercomputer Application (NCSA) at the University of Illinois, Urbana−Champaign, for generous allocation of computing resources. We thank Dr. Stephan Matzinger (University of Fribourg, Switzerland) for the thermochemical calculations and Prof. Thomas Bally (University of Fribourg, Switzerland) and Prof. Paul v. Rague Schleyer (University of Georgia) for valuable discussions.

Supporting Information Available: Energies, zero-point energies, NICS values, and Cartesian coordinates for the computed structures are available. This material is available free of charge via the Internet at http://pubs.acs.org.

References and Notes

(1) (a) Ellinger, L. P. *Polymer* **1964**, *5*, 559. (b) Bell, F. A.; Fugij, R. A.; Ledwith, A. *J. Chem. Soc., Chem. Commun.* **1969**, 251.

(2) For recent overviews compare e.g.: (a) Sancar, A.; Sancar, G. B. *Annu. Rev. Biochem.* **1988**, *52*, 29. (b) Sancar, A. *Biochemistry* **1994**, *33*, 2. (c) Sancar, A. In *Advances in Electron Transfer Chemistry Vol. 2*; Mariano, P. S., Ed.; JAI Press: New York, 1992; p 215. (d) Begley, T. B. *Acc. Chem. Res.* **1994**, *27*, 394.

(3) (a) Bach, R. D.; Schilke, I. L.; Schlegel, H. B. *J. Org. Chem.* **1996**, *61*, 4845. (b) Clark, T. *Acta Chim. Scand.* **1997**, *51*, 646 and references therein.

(4) (a) Gescheidt, G.; Prinzbach, H.; Davies, A. G.; Herges, R. *Acta Chim. Scand.* **1997**, *51*, 171. (b) Prinzbach, H.; Gescheidt, G.; Martin, H. D.; Herges, R.; Heinze, J.; Surya, P. G. K.; Olah, G. A. *Pure Appl. Chem.* **1995**, *67*, 673 and references therein.

(5) (a) Bauld, N. L. In *Advances in Electron Transfer Chemistry Vol. 2*; Mariano, P. S., Ed.; JAI Press: New York, 1992; p 1. (b) Mattes, S. L.; Farid, S. *Org. Photochem.* **1983**, *45*, 233. (c) Bauld, N. L. *Tetrahedron* **1989**, *45*, 5307. (d) Lewis, F. D.; Kojima, M. *J. Am. Chem. Soc.* **1988**, *110*, 8664.

(6) Ono, Y.; Linn, S. H.; Tzeng, W.-B.; Ng, C. Y. *J. Chem. Phys.* **1984**, *80*, 1482 and references therein.

(7) (a) Doepker, R. D.; Ausloos, P. *J. Chem. Phys.* **1965**, *43*, 3814. (b) Doepker, R. D.; Ausloos, P. *J. Chem. Phys.* **1966**, *44*, 1641.

(8) Pabon, R. A.; Bauld, N. L. *J. Am. Chem. Soc.* **1984**, *106*, 1145.

(9) Alvarez-Idaboy, J. R.; Eriksson, L. A.; Fängström, T.; Lunell, S. *J. Phys. Chem.* **1993**, *97*, 12737.

(10) Simkin, B. Y.; Glukhovtsev, M. N. *Zh. Org. Khim.* **1987**, *23*, 2033.

(11) Lee, T.-S.; Lien, M. H.; Jen, S.-F.; Ou, M.-C.; Wu, H.-F.; Gau, Y.-F.; Chang, T.-Y. *J. Mol. Struct. (THEOCHEM)* **1988**, *170*, 121.

(12) (a) Jungwirth, P.; Carsky, P.; Bally, T. *J. Am. Chem. Soc.* **1993**, *115*, 5776. (b) Jungwirth, P.; Bally, T. *J. Am. Chem. Soc.* **1993**, *115*, 5783. These papers also provide excellent overviews over previous studies. For related [2+2] cycloaddition reaction of radical cations, compare: (c) Hrouda V.; Roeselova M.; Bally T. *J. Phys. Chem. A* **1997**, *101*, 3918, and ref 18.

(13) E.g.: (a) Van der Meij, C. E.; VanEck, J.; Niehaus, A. *Chem. Phys.* **1989**, *130*, 325. (b) Hsieh, T.; Gilman, J. P.; Weiss, M. J.; Meisels, G. G. *J. Phys. Chem.* **1981**, *85*, 2722.

(14) Compare also: (a) Ma, N. L.; Smith, B. J.; Radom, L. *Chem. Phys. Lett.* **1992**, *193*, 386. (b) Nobes, R. H.; Moncrieff, D.; Wong, M. W.; Radom, L.; Gill, P. M. W.; Pople, J. A. *Chem. Phys. Lett.* **1991**, *182*, 216. (c) Wiest, O. *J Mol. Struct. (THEOCHEM)* **1996**, *368*, 39. (d) Bally, T.; Borden, W. T. *Rev. Comput. Chem* **1998**, *13*, 1. (f) Haberl, U.; Wiest, O.; Steckhan, E. *J. Am. Chem. Soc.*, in press.

(15) (a) Wiest, O. *J. Am. Chem. Soc.* **1997**, *119*, 5713. Compare also: (b) Sastry, G. N.; Bally, T.; Hrouda, V.; Carsky, P. *J. Am. Chem. Soc.* **1998**, *120*, 9323. (c) Barone V.; Rega N.; Bally T.; Sastry, G. N. *J. Phys. Chem. A* **1999**, *103*, 217.

(16) E. g.: (a) Hrovat, D. A.; Morokuma, K.; Borden, W. T. *J. Am. Chem. Soc.* **1994**, *116*, 1072. (b) Jiao, H.; Schleyer, P. v. R. *Angew. Chem., Int. Ed. Engl.* **1995**, *34*, 334.

(17) Wiest, O.; Houk, K. N. *Top. Curr. Chem.* **1996**, *183*, 1.

(18) (a) Hrouda, V.; Carsky, P.; Ingr, M.; Chval, Z.; Sastry, G. N.; Bally, T. *J. Phys. Chem. A* **1998**, *102*, 9297. (b) Hrouda, V.; Roeselova, M.; Bally T. *J. Phys. Chem. A* **1997**, *101*, 3925.

(19) E. g.: (a) Adamo, C.; Barone, V.; Fortunelli, A. *J. Chem. Phys.* **1995**, *102*, 384. (b) Lim, M. H.; Wothington, S. E.; Dulles, F. J.; Cramer, C. J. In *Chemical Applications of Density Functional Theory*; Laird, B. B., Ross, R. B., Ziegler, T., Eds.; ACS Symposium Series 629; American Chemical Society: Washington, DC, 1996; pp 402.

(20) (a) Bally, T.; Sastry, G. N. *J. Phys. Chem. A* **1997**, *101*, 7923. (b) Braida, B.; Hiberty, P. C.; Savin, A. *J. Phys. Chem. A* **1998**, *102*, 7872. (c) Sodupe, N.; Bertran, J.; Rodriguez-Santiago, L.; Baerenz, E. J. *J. Phys. Chem. A* **1999**, *103*, 166.

(21) *Gaussian 94*, Revision D.2 M; Frisch, J.; Trucks, G. W.; Schlegel, H. B.; Gill, P. M. W.; Johnson, B. G.; Robb, M. A.; Cheeseman, J. R.; Keith, T.; Petersson, G. A.; Montgomery, J. A.; Raghavachari, K.; Al-Laham, M. A.; Zakrzewski, V. G.; Ortiz, J. V.; Foresman, J. B.; Peng, C. Y.; Ayala, P. Y.; Chen, W.; Wong, M. W.; Andres, J. L.; Replogle, E. S.; Gomperts, R.; Martin, R. L.; Fox, D. J.; Binkley, J. S.; Defrees, D. J.; Baker, J.; Stewart, J. P.; Head-Gordon, M.; Gonzalez, C.; Pople, J. A. Gaussian, Inc.: Pittsburgh, PA, 1995.

(22) Ushida, K.; Shida, T.; Iwasaki, M.; Toriyama, K.; Numone, K. *J. Am. Chem. Soc.* **1983**, *105*, 5496. After annealing at 77 K and refreezing to 4 K, a third hpcc of 5 G could be resolved.

(23) Genaux, C. T.; Kern, F.; Walters, W. D. *J. Am. Chem. Soc.* **1953**, *75*, 6196.

(24) Calculated from the combution enthalpy of cyclobutane of −650.22 ± 0.1 kcal/mol, the heat of formation of ethylene of 12.54 kcal/mol, the ionization potential of cyclobutane of 9.82 ± 0.05 eV and the ionization potential of ethylene of 10.5138 ± 0.0006 eV. (a) Holmes, J. L.; Lossing, F. P. *Org. Mass. Spectrom.* **1991**, *26*, 537. (b) Chase, M. W., Jr. *J. Phys. Chem. Ref. Data* **1998**, *Monograph 9*, 1. (c) Williams, B. A.; Cool, T. A. *J. Phys. Chem.* **1991**, *94*, 6358. (d) Kaarsemaker, S.; Coops, J. *Recl. Trav. Chim. Pays-Bas*, **1952**, *71*, 261. (e) Coops, J.; Kaarsemaker, S. J. *Recl. Trav. Chim. Pays-Bas* **1950**, *69*, 1364. Compare, however, also the reaction enthalpy of the cycloreversion of neutral cyclobutane of 20.7 ± 1.0 kcal/mol. (f) Quick, L. M.; Knecht, D. A.; Back, M. H. *Int. J. Chem. Kinet.* **1972**, *4*, 61.

(25) Matzinger, S., personal communication.

(26) Bernardi, F.; Bottoni, A.; Robb, M. A.; Schlegel, H. B.; Tonachini, G. *J. Am. Chem. Soc.* **1985**, *107*, 2260.

(27) Burdi, D.; Begley, T. *J. Am. Chem. Soc.* **1991**, *113*, 7768.

(28) Doubleday, C., Jr. *J. Am. Chem. Soc.* **1993**, *115*, 11968.

(29) Schleyer, P. v. R.; Maerker, C.; Dransfeld, A.; Jiao, H.; van Eikema Hommes, N. J. R. *J. Am. Chem. Soc.* **1996**, *118*, 6317.

(30) Schepp, N. P.; Johnston, L. J. *J. Am. Chem. Soc.* **1994**, *116*, 6895.